Development 115, 973-987 (1992)
Printed in Great Britain © The Company of Biologists Limited 1992

Differential distribution patterns of CRABP I and CRABP II transcripts during mouse embryogenesis

ESTHER RUBERTE[1,†], VALÉRIE FRIEDERICH[1], GILLIAN MORRISS-KAY[2] and PIERRE CHAMBON[1,*]

[1]*Laboratoire de Génétique Moléculaire des Eucaryotes, CNRS, U. 184 de Biologie Moléculaire et de Génie Génétique, INSERM, Institut de Chimie Biologique, Faculté de Médecine 11, rue Humann, 67085 Strasbourg Cédex, France*
[2]*University of Oxford, Department of Human Anatomy, South Parks Road, Oxford, UK*

*To whom all correspondence should be addressed
†Present address: University of Oxford, Department of Human Anatomy, South Parks Road, Oxford, UK

Summary

We have compared the transcript distribution of cellular retinoic acid binding protein (CRABP) I and II genes in mouse embryos at various stages of development. Both CRABP transcripts are present in embryonic structures from the earliest stages studied and exhibit specific patterns of distribution, suggesting that the two retinoic acid (RA) binding proteins perform different functions during mouse embryogenesis. The CRABP I transcript distribution correlates well with structures known to be targets of excess retinoid-induced teratogenesis (e.g. neural crest cells and hindbrain), suggesting that cells expressing CRABP I are those that cannot tolerate high levels of RA for their normal developmental function. The embryonic structures expressing CRABP II transcripts include those structures that have been shown to be adversely affected by excess of retinoids, such as limbs and hindbrain, but CRABP II transcripts are also found in structures not known to be specifically vulnerable to raised RA levels. The CRABP II gene is coexpressed with retinoic acid receptor (RAR)-β and cellular retinol binding protein (CRBP) I genes in a number of tissues such as the gut endoderm, hypophysis and interdigital mesenchyme, all of which are devoid of CRABP I transcripts. Interestingly, the expression of the three genes, RAR-β, CRABP II and CRBP I, is induced by retinoic acid, which suggests a link between the synthesis of RA from retinol and the control of expression of subsets of RA-responsive genes. The transcript distribution of CRABP I and II is discussed in relation to the teratogenic effects of RA, and compared to the RA-sensitive pattern of expression of other important developmental genes.

Key words: cellular retinoic acid binding proteins, mouse embryo development, in situ hybridization, mRNA distribution.

Introduction

Vitamin A (retinol) and its active metabolite retinoic acid (RA) play important roles during mammalian morphogenesis. In mammals retinoids are well known to be potent teratogenic agents in both deficiency and excess (Lammer et al., 1985; Morriss, 1972; Rosa et al., 1986; Shenefelt, 1972; Warkany et al., 1943; Wilson et al., 1953). RA exerts its effects by binding to nuclear receptors (RARs) that modulate the transcriptional activity of specific target genes (Benbrook et al., 1988; Brand et al., 1988; Giguère et al., 1987; Krust et al., 1989; Petkovich et al., 1987; Zelent et al., 1989). In addition to the nuclear receptors, there exist two cytosolic RA binding proteins, the cellular retinoic acid binding proteins I (CRABP I) and II (CRABP II) (Blomhoff et al., 1990; Giguère et al., 1990; Stoner and Gudas, 1989). The two CRABP proteins are structurally very similar, but the affinity of CRABP II for RA appears to be lower than that of CRABP I (for a review see Chytil and Stump, 1991). It has been proposed that the CRABPs could transport RA from the cytoplasm to the nucleus where it would be transferred to the nuclear receptors (Takase et al., 1979, 1986). Alternatively, it has been suggested that the role of CRABPs could be controlling the actual concentration of free RA in a given cell (Boylan and Gudas, 1991; Maden et al., 1988; Robertson, 1987; Ruberte et al., 1991; Smith et al., 1989). Maden et al. (1988) have described a graded distribution of CRABP I in the chick limb bud, with the highest levels in the anterior margin of the limb, thus opposite to the putative concentration gradient of total RA, in such a way that the presence of CRABP may result in a steeper gradient of free RA available for binding to RARs. In agreement with this hypothesis, Boylan and Gudas (1991) have reported that overexpression of CRABP I in F9 cells results in reduced RA-induced activation of transcription by RARs, suggesting that the amount of RA that reaches the nucleus is decreased.

We have previously described the pattern of distribution of CRABP I transcripts in mouse embryos (Dollé et al., 1989b, 1990; Ruberte et al., 1991). To investigate the role

that the two binding proteins may play in the transduction of the RA signal, we have now compared the transcript distribution of the two CRABPs at different stages of mouse development. Both transcripts are present in embryonic structures from the earliest stages studied, but they exhibit different patterns of distribution. The results are discussed in relation to RA-induced abnormalities and to the patterns of expression of genes that appear to have an important role in the transduction of the RA signal during normal development.

Materials and methods

^{35}S-labelled RNA probes were synthesized using T7-polymerase (according to the suppliers directions, Promega Biotec) from full length cDNAs coding for CRABP I (Stoner and Gudas, 1989; Dollé et al., 1989b) and CRABP II (Giguère et al., 1990, a gift of Ph. Kastner) cloned in an antisense orientation into Bluescript SK+ after linearization with *Eco*RI. Probe length was reduced to an average of 150 nucleotides by limited alkaline hydrolysis, as described by Ruberte et al. (1990).

The distribution of CRABP I and II transcripts was analyzed by in situ hybridization on mouse embryo sections from day 8 to 14.5. Brains from 18.5-day foetuses were dissected out from skulls.

Recovery and paraffin embedding of mouse embryos, in situ hybridization, emulsion autoradiography and staining of histological sections were performed as previously described (Ruberte et al., 1990). The time of autoradiographic exposure was 7 days for the CRABP I probe and 10-12 days for the CRABP II probe.

Results

At every stage analyzed, consecutive sections were hybridized with CRABP I and II probes in order to compare their transcript distribution. CRABP II transcripts exhibited a wider distribution than CRABP I transcripts among the various embryonic tissues; however, within a given tissue the relative amount of transcripts was in general higher for the CRABP I gene as reflected by the shorter time of autoradiographic exposure. The CRABP I transcript distribution has already been described in detail (Dollé et al., 1989b, 1990; Ruberte et al., 1991) and only some particularly interesting and comparative aspects will be presented here.

CRABP II transcripts at early morphogenetic stages

At the 5-somite stage (early day 8), CRABP II transcripts were detected in the neural epithelium at all levels of the craniocaudal axis (Figs 1A, B and 2A to C). This is in contrast to the distribution of CRABP I transcripts at this stage which were absent from the forebrain (Fig. 2A, C, see also Ruberte et al., 1991). Only diffuse labelling was observed with the CRABP II probe in the cranial mesenchyme, whereas a more intense signal was detected in the undifferentiated presomitic mesenchyme, where CRABP I transcripts were also present (Figs 1A, B and 2A, C, see also Ruberte et al., 1991).

In 8.5-day embryos, the first pharyngeal arches are present. The major mesenchymal component of the pharyngeal arches and frontonasal mesenchyme is derived from the neural crest (Noden, 1978a, b). The migrating neural crest cells, which contained high levels of CRABP I transcripts (Fig. 1C, arrow), were not labelled with the CRABP II probe. The mesenchyme of the pharyngeal arches and of the frontonasal region showed a faint labelling with the CRABP II probe compared to the intense labelling with the CRABP I probe in these structures (Fig. 1C). In contrast, the neural crest cell-derived cranial ganglia contained high levels of both CRABP I and CRABP II transcripts (Fig. 1C, see the trigeminal ganglion anlage). In the neural epithelium, CRABP II transcripts were particularly abundant in the hindbrain and trunk regions, and were also present in the forebrain (Fig. 1C). The most caudal parts of the neural tube and the tail bud showed a signal slightly above the background (not shown). This is in contrast to the more restricted pattern of expression of the CRABP I gene which is not expressed in the forebrain or at post-cervical levels of the trunk neural tube (Fig. 1C and Ruberte et al., 1991). CRABP II transcripts in these embryos were also detected in the ventral endoderm of the pharyngeal pouches, foregut and midgut, where no CRABP I transcripts were detected (Fig. 1C and data not shown). Both CRABP I and II transcripts were present in the somatopleure, but were absent from the splanchnopleure (Fig. 1C).

From day 9 of gestation, high levels of CRABP II transcripts were found in the mandibular and frontonasal mesenchyme when compared to the diffuse labelling observed at previous stages (Fig. 1D; compare with 1C). CRABP I transcripts were also present in the same regions. CRABP II, but not CRABP I transcripts were detected in the lateral and tail bud mesenchyme, and in the foregut and midgut endoderm as at the previous stage (Fig. 1D and data not shown). In day 9 embryos, the otic vesicle was labelled with the CRABP II probe, but showed no CRABP I transcripts (Figs 1D, 2E). The subpopulations of neural crest cells that later form the cranial ganglia were intensely labelled with both the CRABP I and II probes (Fig. 1D, arrows, and Ruberte et al., 1991).

CRABP I and II transcripts in developing rhombomeres

CRABP I and II transcripts also showed a differential pattern of distribution in the developing rhombomeres at the different stages analyzed. A diagrammatic representation of CRABP I and II transcript distribution in rhombomeres and derived neural crest cells at three different stages of development is shown in Fig. 11. At the 4- to 7-somite stage, four primary rhombomeres are recognized, rhombomeres A, B (otic rhombomere), C and D (occipital rhombomere) (Adelmann, 1925; Bartelmez, 1923; Müller and O'Rahilly, 1985; O'Rahilly and Müller, 1987, see Fig. 11). The preotic sulcus, which is located between rhombomeres A and B, marks the boundary between the rostral and caudal hindbrain. During subsequent development, rhombomere A subdivides into rhombomere A1 and rhombomere 3. At the 5-somite stage, transcripts of both CRABPs were present caudal to the preotic sulcus (Fig. 2A, see also Ruberte et al., 1991). CRABP I transcripts were most abundant in a small portion of the caudal hindbrain, immediately caudal to the preotic sulcus, whereas CRABP II expression was highest in more caudal regions and extended further

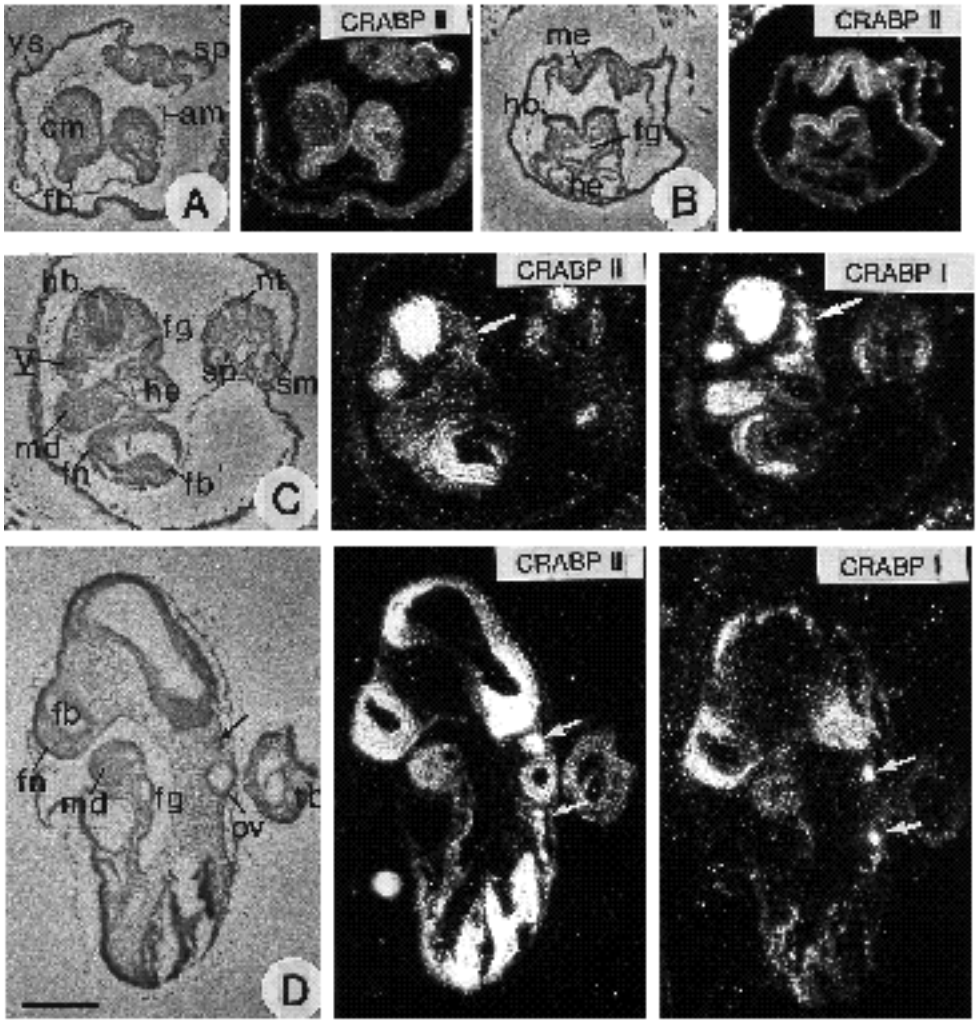

Fig. 1. (A and B) Transverse sections through a day-8 embryo (10-somite stage) showing the distribution of CRABP II transcripts at forebrain/midbrain (A) and hindbrain (B) levels. The very bright spots on the right upper corner of A are due to the refraction of blood cells and are not a hybridization signal. (C) Consecutive transverse sections through forebrain, hindbrain and trunk levels of a 8.5-day embryo hybridized with the CRABP I and CRABP II probes. Note the differences in labelling of the migrating neural crest cells (white arrows), the pharyngeal arch and frontonasal mesenchyme, and the forebrain neuroepithelium. (D) Parasagittal section of a day 9 embryo. Note the differences in the staining of the brain vesicles, mandibular arch and otic vesicle. The cranial ganglia are labelled with both CRABP I and II probes (white and black arrows). am, amnion; cm, cranial mesenchyme; fb, forebrain; fg, foregut; fn, frontonasal mesenchyme; hb, hindbrain; he, heart; md, mandibular arch; me, presomitic mesenchyme; nt, neural tube; ov, otic vesicle; sm, somatopleure; sp, splanchnopleure; tb, tail bud; ys, yolk sac; V, trigeminal ganglion. Bar, 250μm.

caudally (Fig. 2A). At the 7- to 10-somite stage, CRABP I transcripts were found most abundantly expressed in rhombomere B (the otic rhombomere), and levels of transcripts progressively decreased towards more rostral levels of the neuroepithelium, being lowest in the midbrain and absent from the forebrain regions (Fig. 2B and C). Neural crest cells containing high levels of CRABP I transcripts were seen migrating from levels immediately rostral to the otic placode (not shown, see Ruberte et al., 1991). A relatively intense signal was also observed at the basal side of the neuroepithelium rostral to the preotic sulcus (Fig. 2B). CRABP I-labelled neural crest cells were seen migrating from neuroepithelium rostral to the preotic sulcus to invade the first pharyngeal arch (not illustrated, see Ruberte et al., 1991). Caudal to the otic rhombomere, CRABP I transcripts were found up to the level of the first occipital somites, including undifferentiated epiblast (Fig. 2C, see also Ruberte et al., 1991). CRABP II expression at 7- to 10-somite stage was highest in the neuroepithelium immediately caudal to the otic placode (rhombomere C), and in contrast to CRABP I expression, transcripts were present at all levels in the cranial neuroepithelium, including forebrain, as well as in levels caudal to the occipital somites (Fig. 2B and C). Only a faint signal was detected in the migrating neural crest cells (not shown). The otic placodes were labelled with both probes at these stages (Fig. 2B).

At later stages rhombomere A1 subdivides into rhombomeres 1 and 2, rhombomere B gives rise to rhombomeres 4 and 5, rhombomere C gives rise to rhombomeres 6 and 7, and rhombomere D, which corresponds to the occipital region and lies opposite to the first four pairs of somites, is then called rhombomere 8 (Müller and O'Rahilly, 1985; O'Rahilly and Müller, 1987). At the 12- to 14-somite stage, six rhombomeres are easily recognizable in the embryonic hindbrain. At this stage, CRABP I was detected in all the rhombomeres (Fig. 2D). Rhombomeres 1 to 3 showed the lowest levels of CRABP I transcripts, the levels being highest in rhombomere 4 from which neural crest cells have emigrated (Fig. 2D). Rhombomeres 5 and 6 also expressed high levels of CRABP I and the intensity of the signal progressively decreased in more caudal levels of the neural epithelium. Neural crest cells adjacent to rhombomeres 1, 2 and 6 to 8 were also observed to express CRABP I transcripts (Fig. 2D, white triangles). CRABP II transcripts at this stage were also abundant, but less than for CRABP I, in rhombomere 4 and its derived neural crest cells (Fig. 2D), but not in the crest cells adjacent to rhombomeres 6-8 (Fig. 2D, white triangles). High levels of CRABP II tran-

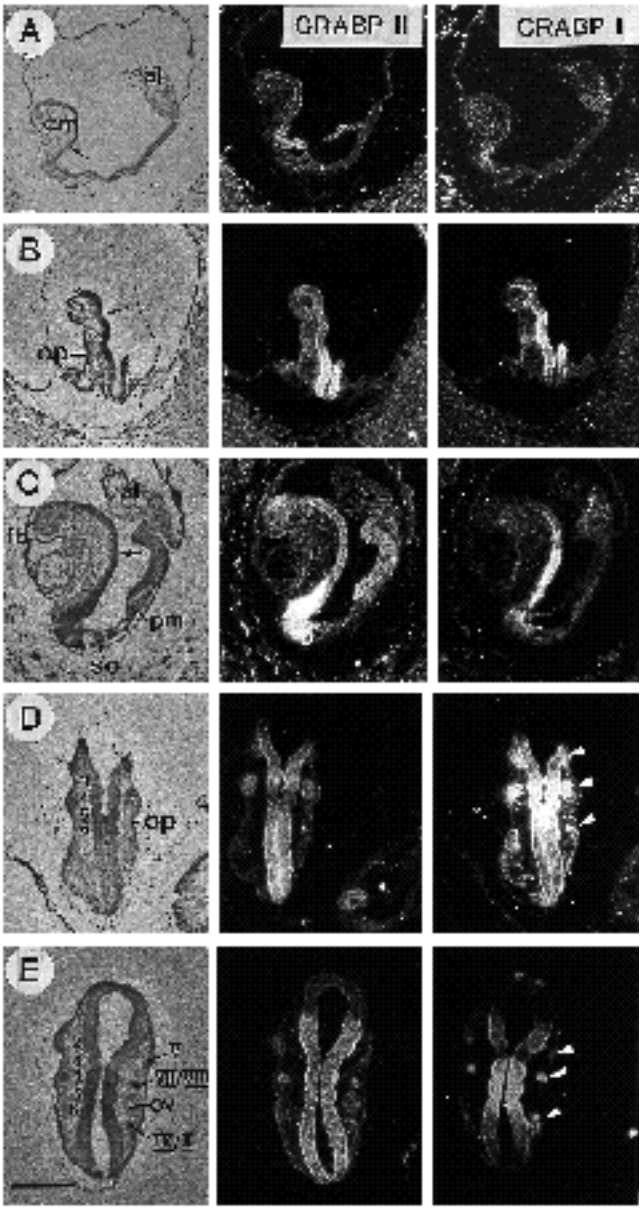

Fig. 2. Sections of mouse embryos at different developmental stages to show the transcript distribution of CRABP I and II in the developing rhombomeres (2 to 6 in panel E). (A) Parasagittal sections of a 5-somite embryo. (B) Coronal sections through the hindbrain neuroepithelium of a 7-somite embryo. (C) Parasagittal sections of a 10-somite embryo. (D) Coronal sections of a 12-somite embryo through the hindbrain neuroepithelium. (E) Coronal sections through the hindbrain of a 18- to 19-somite embryo. The arrows in A-C point to the preotic sulcus. al, allantois; cm, cranial mesenchyme; fb, forebrain; op, otic placode; ov, otic vesicle; pm, presomitic mesenchyme; so, occipital somites; VI, VII/VIII and IX/X, cranial ganglia. Bar, 250μm.

scripts were also observed in rhombomeres 7, 8 and in more caudal levels of the neural epithelium. Rhombomeres 1 to 3 and 6 were also labelled with the CRABP II probe although less intensely, as were the neural crest cells migrating from rhombomere 2. The weakest signal was detected in rhombomere 5, opposite the invaginating otic placode.

At the 18- to 19-somite stage (9 days), all rhombomeres were labelled with both CRABP probes (Fig. 2E). CRABP I transcripts were most abundant in rhombomeres 4 to 6, and the intensity of the signal progressively decreased rostrally and caudally. However, only the most dorsal regions of the neural epithelium of rhombomere 3 appeared to express CRABP I transcripts (Fig. 2E and data not shown). CRABP II transcripts were found in all rhombomeres, the midbrain showing lower levels of transcripts (Fig. 2E). At this stage the neural crest cells of the trigeminal (V) ganglion and acoustico-facial (VII/VIII) ganglion complex, which migrate from rhombomeres 1-2 and 4, respectively, showed CRABP I and II transcripts. The neural crest cells that will contribute to cranial ganglia IX and X (derived from rhombomeres 6 and 7) also appeared to express both CRABP I and II transcripts, although the signal was relatively weak because these cells form a less condensed cluster than those derived from rhombomeres 2 and 4 (Fig. 2E, white triangles).

CRABP II transcripts in the developing limbs

The forelimb buds become visible on day 9 of gestation, and the hindlimb buds on day 9.5. The limb buds of late day 9.5 embryos showed CRABP I and II transcripts rather homogeneously distributed throughout the mesenchyme (not shown, see Ruberte et al., 1991). The lateral mesenchyme was also labelled. In day 10.5 embryos, CRABP I and II transcripts were present in the mesenchyme of the fore- and hindlimbs (Figs 3, 4A, and 5B, C). In the less differentiated hindlimbs, transcripts of both CRABPs still showed a rather homogeneous distribution in the mesenchymal cells (Fig. 5C). In the forelimbs, the two probes gave a different pattern of transcript distribution. The ectoderm showed no labelling with the CRABP I probe, and only the most dorsal cells of the apical ectodermal ridge (AER) were labelled (not illustrated, see Dollé et al., 1989b). In the ectoderm and the AER, no labelling above the background could be detected with the CRABP II probe.

Alternate dorsoventral sections at different levels perpendicular to the forelimb anteroposterior axis were hybridized with the CRABP probes (Fig. 3). Panel A corresponds to the most anterior sections; however, since the planes of the sections are slightly oblique, the left limb (L) is always cut more anteriorly than the right (R) one. We could not detect any gradient of CRABP II transcripts in the anteroposterior axis of the limbs at this developmental stage (Fig. 3A to D). However, there was a clear dorsoventral difference in the labelling intensity of CRABP II transcripts, lower levels being present ventrally (V) than dorsally (D). Moreover, the most distal mesenchyme (progress zone) cells, which are proliferating actively under the influence of the AER (Summerbell and Lewis, 1975), were only weakly labelled with the CRABP II probe (Figs 3, 4A). CRABP I transcripts at this stage were more abundant in the distal regions of the limb buds, and particularly in the anterior region were absent from the more proximal central and dorsal mesenchyme (Figs 3, 5C, see also Dollé et al. 1989b).

At day 12.5 of development, the limbs are paddle shaped and the first precartilaginous condensations have appeared. At this stage, CRABP II transcripts were widely distributed

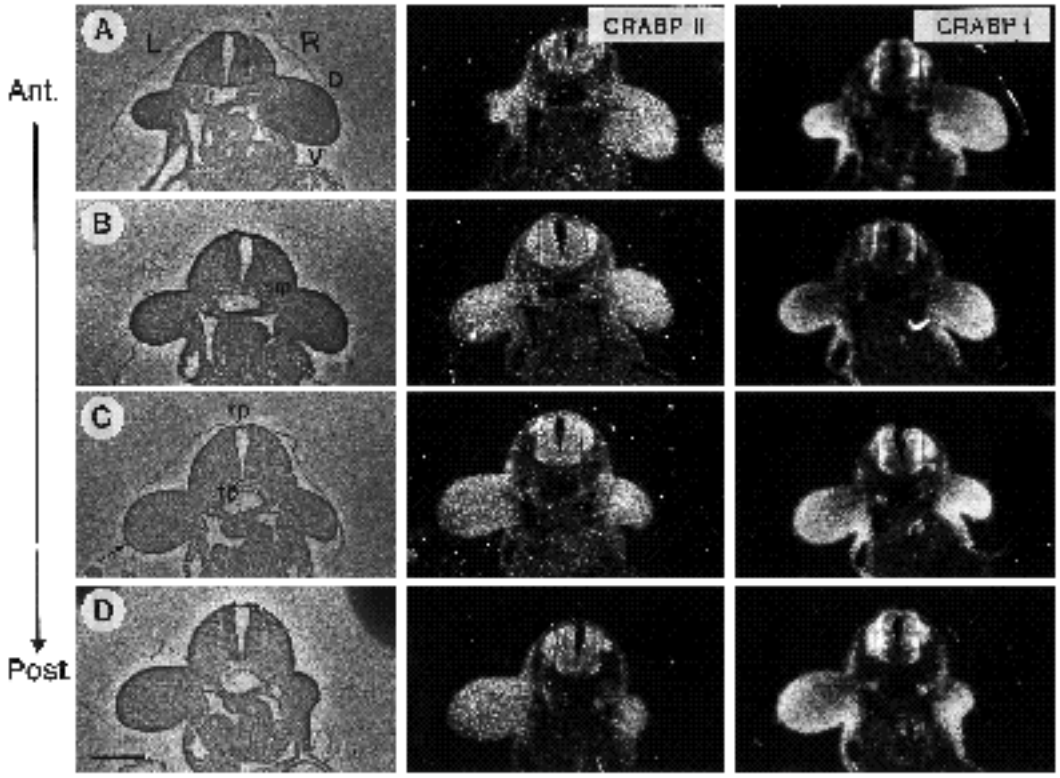

Fig. 3. Serial transverse sections across the forelimb level of a day 10.5 embryo. Consecutive sections have been hybridized with the CRABP I and II probes. Since the plane of the sections is slightly oblique the left limb represents a more anterior plane of section than the right limb. The arrow in C points to the AER. Ant, anterior; Post, posterior; L, left; R, right; D, dorsal; V, ventral; fp, floor plate; m, motoneurons; rp, roof plate. Bar, 250μm.

in the limb mesenchyme, but were absent from the precartilaginous condensations and differentiated cartilage (data not shown). CRABP I transcripts were similarly excluded from the precartilaginous condensations and cartilages; however, CRABP II transcripts were widely distributed in the presumptive non-chondrogenic mesenchyme of the limbs, whereas CRABP I transcripts were more restricted to the periphery (data not shown).

At 13.5 days of gestation, the skeletal elements consist of cartilage and the musculature is differentiating. At this stage, CRABP II transcripts were clearly seen in the developing muscles and interdigital mesenchyme where they were coexpressed with RAR-β and CRBP I, but were absent from the cartilage that expressed RAR-γ transcripts (Fig. 4B). Note, however, that RAR-β was not expressed in the distal mesenchyme underlying the AER at the tip of the digits whereas CRABP II, CRBP I and CRABP I were coexpressed in these sites. CRABP I transcripts at this stage were absent from the cartilage and developing muscles, but high levels of transcripts were found in parts of the perichondrium and mesenchyme (Fig. 4B). At 14.5 days CRABP I and II transcripts were also found in the connective tissues (tendons, ligaments and perichondrium) (data not shown, see also Dollé et al., 1989b, 1990).

CRABP II transcripts in the somitic derivatives

The sclerotome, myotome and dermatome derivatives of the somites were observed in appropriate sections of embryos aged from 9.5 to 13.5 days of gestation. At all stages CRABP II transcripts were particularly abundant in the dermamyotome portion (Figs 5, 7C) as well as in the differentiating skeletal muscle (Figs 4B, 10C). Sclerotome cells were also labelled although less intensely (Figs 5B, 6). This was lost prior to chondrogenesis, and no significant levels were found in either somite-derived (see the vertebra in Fig. 9C) or non-somite-derived cartilage (Fig. 4B). CRABP I transcripts were low in the somites and their derivates and were restricted to a small portion of the dermamyotome (Figs 5, 7C).

CRABP II transcripts in craniofacial structures

As described above, high levels of CRABP II transcripts were present in the pharyngeal arch mesenchyme and pharyngeal pouch endoderm from day 9 of gestation, whereas no labelling was observed in the ectodermal layer. CRABP I transcripts were present in specific subpopulations of the cranial mesenchyme and neural epithelium, but not in the surface ectoderm or pharyngeal endoderm (Fig. 1D).

At day 10.5, abundant CRABP II expression was still seen in frontonasal (Fig. 5) and pharyngeal arch mesenchyme (Fig. 5C). The surface ectoderm showed no significant labelling with the CRABP II probe, but a signal was detected in the olfactory placodes, which are neuroectodermal derivatives (Couly and Le Douarin, 1987) (Fig. 5A and B). CRABP I transcripts at this stage were particularly abundant in the distal portion of the frontonasal and

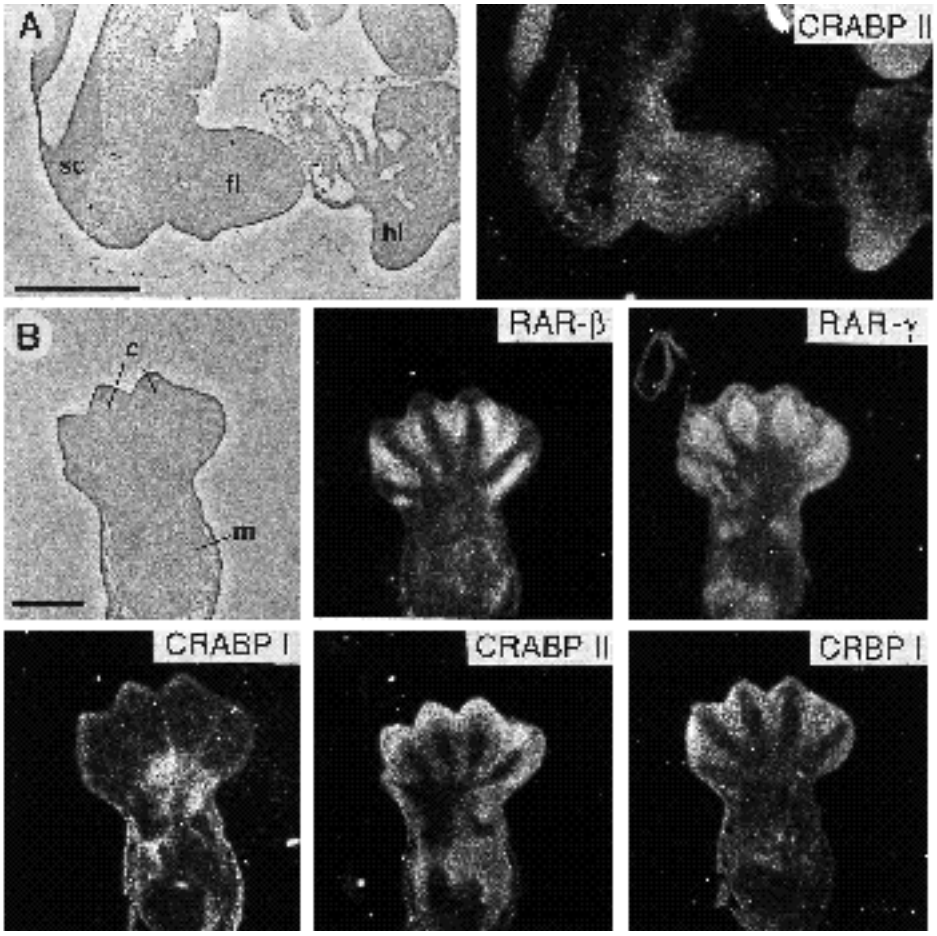

Fig. 4. (A) Parasagittal section through the forelimb of a 10.5 day embryo showing the low amount of CRABP II transcripts in the distal tip of the forelimb. (B) Sections through a 13.5 day hindlimb hybridized with the RAR-β, RAR-γ, CRABPs and CRBP I probes. c, cartilage; fl, forelimb; hl, hindlimb; m, muscle; sc, spinal cord. Bar, 250μm.

pharyngeal arch mesenchyme (Fig. 5C and Dollé et al., 1990). Neither the surface ectoderm nor the olfactory placodes showed CRABP I transcripts at this developmental stage (Fig. 5A, B).

At day 12.5, CRABP II transcripts were abundant in the distal frontonasal mesenchyme, in the mandible and in the tongue, in a distribution overlapping, but not identical to that of CRABP I transcripts (Figs 6, 7A, 9B).

From day 13.5 onwards, CRABP II transcripts were detected in the muscles and in the perichondrium of the facial skeletal elements, and CRABP I transcripts were detected in the mesenchyme surrounding the cartilaginous structures (data not shown). Thus the late distribution of CRABP I and II transcripts in the skeletal elements and muscles of the face, and more generally in the whole body, was similar to that previously described in the limbs (Fig. 4B, see also Dollé et al., 1990; Ruberte et al., 1992).

From day 12.5, CRABP II transcripts were also detected in the developing thymus, which appeared to be devoid of CRABP I transcripts (Fig. 7A, B).

CRABP II transcripts in the urogenital system

At day 10.5, CRABP II transcripts were detected in the mesenchyme and tubules of the mesonephros (Figs 5B, 7C). CRABP I transcripts were in contrast restricted to the dorsal mesenchyme of the mesonephros (Fig. 7C, see also Dollé et al., 1990). At day 12.5, the mesonephros contains many regressing mesonephric tubules and the metanephros is differentiating. At this stage, CRABP II transcripts are no longer expressed in the mesonephros, but they are present in the developing metanephros (Fig. 7D, arrow). CRABP I transcripts were detected in the mesenchymal cells surrounding the developing metanephros (Fig. 7D, arrow). At day 14.5, CRABP II transcripts were more generally distributed than those of CRABP I, and were present in both the stromal cells and nephrogenic tubules of the kidney, whereas CRABP I transcripts were present only in the stromal cells (Fig. 7E).

CRABP II transcripts were also detected at 12.5 days in the periphery of the genital tubercle mesenchyme in a distribution similar to that found with the CRABP I probe, but unlike CRABP I, were also present at low levels in the core mesenchyme of this structure (Fig. 7D). This mesenchymal labelling persisted at later developmental stages.

CRABP II transcripts in neural structures

CRABP II transcripts were found in the neural epithelium from the earliest stage analyzed (see above and Figs 1, 2A-C). At days 9 to 10.5, CRABP II transcripts were present in all of the brain vesicles although they were not homogeneously distributed (see Fig. 1D). In general the floor plate and ventral regions of the neural epithelium of the brain showed low levels of CRABP II transcripts (Figs 1D, 5C). It is interesting to note that CRABP I transcripts were

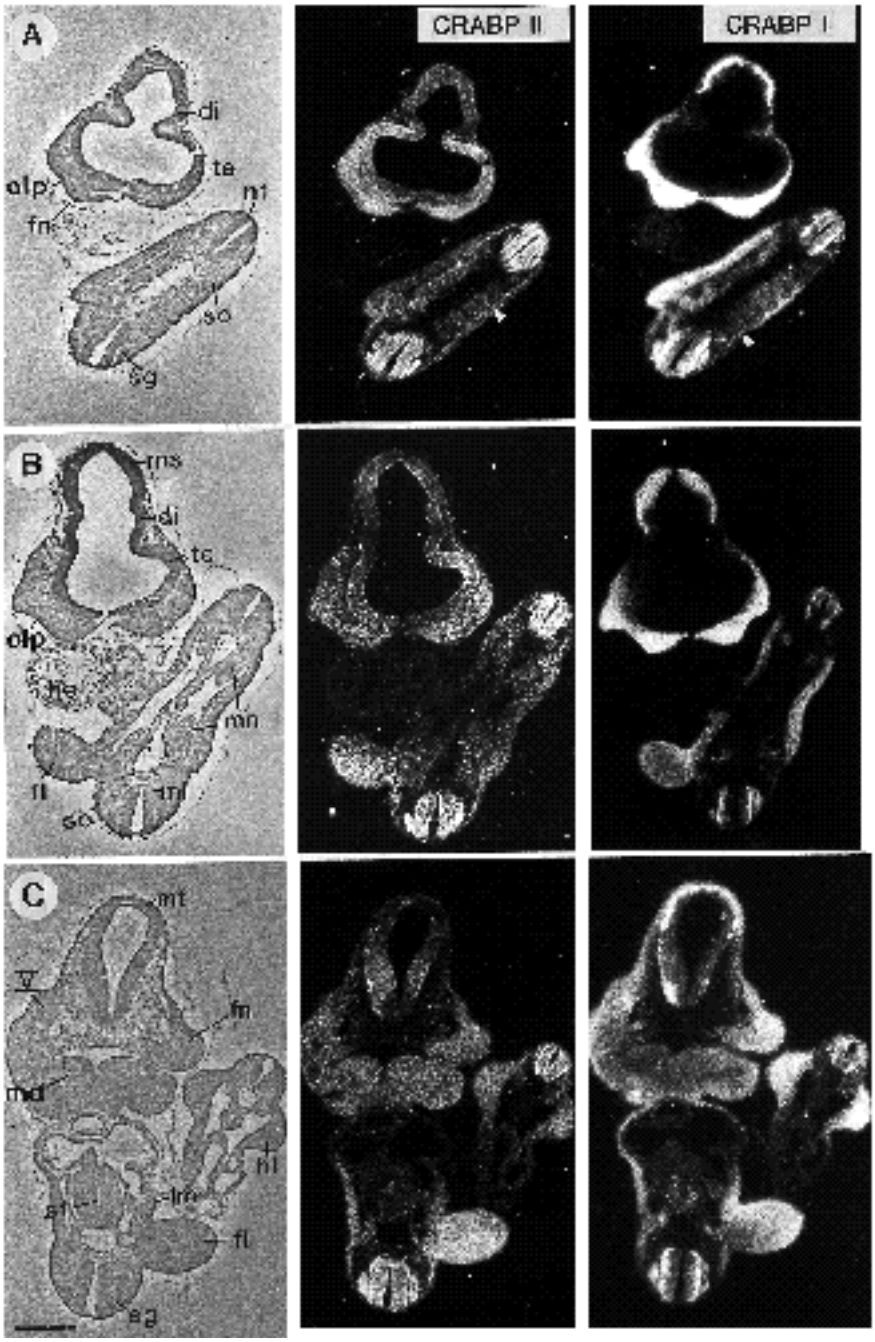

Fig. 5. Serial frontal sections through a 10.5-day embryo. Consecutive sections have been hybridized with the CRABP I and II probes. (A and B) The myotomic portions of the somites are more intensely labelled with both CRABP probes (arrowheads). Note that only CRABP II transcripts are detected in the forebrain and in the olfactory placodes. (B and C) These sections show the differential intensity of the signal between the ventral and dorsal portions of the forelimb buds with the CRABP II probe, compared with the more homogeneous distribution of transcripts in the less differentiated hindlimb buds, and the different pattern of transcript distribution of the CRABP I gene. di, diencephalon; fl, forelimb; fn, frontonasal mesenchyme; he, heart; hl, hindlimb; lm, lateral mesenchyme; md, mandibular arch; ml, mantle layer; mn, mesonephros; ms, mesencephalon; mt, metencephalon; nt, neural tube; olp, olfactory placode; sg, spinal ganglia; so, somite; st, stomach; te, telencephalon; V, trigeminal ganglion. Bar, 500μm.

absent from the telencephalon and diencephalon at these developmental stages (Fig. 5A, B), and no transcripts were detected in the floor and roof plates of the neural tube (Figs 3, 5). As at previous stages, CRABP I transcripts were absent from the forebrain, and labelling of the mesencephalon was restricted to the outermost cells (Fig. 5A, B).

At days 12.5 and 13.5, CRABP II transcripts were widely distributed in the brain, but several regions showed a particularly intense signal (Figs 6, 7A, 9B). CRABP II transcripts were present in the telencephalic regions (Figs 6, 9B) and around the optic stalk (Fig. 6). The lateral walls and the mantle layer of the diencephalon were also labelled (data not shown). Homogeneous labelling was observed in the mesencephalon with the CRABP II probe, whereas only the outermost cells appeared to contain CRABP I transcripts (Fig. 6). In the metencephalon and myelencephalon, the cells in the mantle layer were more intensely labelled with the CRABP II probe than those of the neuroepithelial and marginal layers, and also showed some labelling with the CRABP I probe (Figs 6, 7A and data not shown). At 13.5 days, CRABP I transcripts were also detected in the striatum where no CRABP II transcripts were found (data not shown).

From 14.5 days, CRABP II transcripts were detected in the cerebral hemispheres, in the thalamus (Fig. 8A, B), in the motor nuclei of the trigeminal and facial nerves, in the

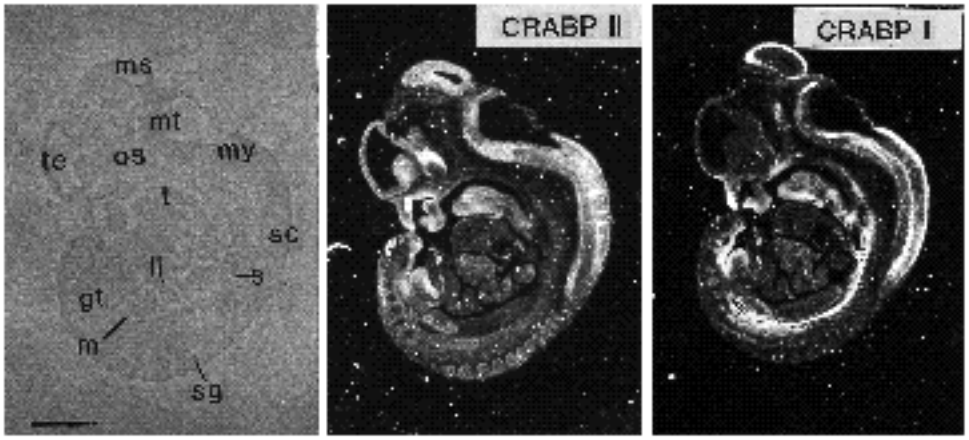

Fig. 6. Parasagittal sections of a 12.5-day embryo. All the brain vesicles and the spinal cord show CRABP II transcripts, whereas CRABP I transcripts are absent from the telencephalon and diencephalon. Labelling is also seen in the spinal ganglia with the CRABPII probe. CRABP I and II transcripts are detected in the genital tubercle as well as in the developing metanephros. Diffuse labelling with the CRABP II probe is detected in the liver. gt, genital tubercle; li, liver; m, metanephros; ms, mesencephalon; mt, metencephalon; my, myelencephalon; os, optic stalk; s, sclerotomes; sc, spinal cord; sg, spinal ganglia; t, tongue; te, telencephalon. Bar, 1mm.

pontine region (Fig. 8A and data not shown) and in the dorsal efferent nucleus of the vagus nerve (Fig. 8C). CRABP I transcripts were detected in the striatum, hippocampus, medulla oblongata and pons (not shown).

In the spinal cord, CRABP II transcripts were first homogeneously distributed in the trunk neural tube (Fig. 1C). After differentiation into basal (motor) and alar (sensory) plates, the transcript distribution became more restricted. At day 10.5, slightly higher levels of CRABP II transcripts were detected in the presumptive motor columns when compared to the rest of the neural tube (Fig. 3 and data not shown). CRABP I transcript distribution was more restricted and transcripts were preferentially found in the marginal and mantle layers (Figs 3, 5). At day 13.5, CRABP II transcripts were detected in the presumptive motor columns of the basal plate and in the newly formed neuroblasts in the alar plate. CRABP I transcripts, in contrast, were preferentially expressed in the alar plate of the spinal cord (Fig. 9C). The neuroepithelial layer and the floor and roof plates showed neither CRABP II nor CRABP I transcripts at this stage (Fig. 9C).

CRABP II transcripts were detected in the cranial and spinal ganglia at every stage analysed (e.g. Figs 1, 5, 6, 9C). The cranial ganglia also showed CRABP I transcripts throughout this period (Fig 1C, D, and 2E), but, in contrast, the spinal ganglia were labelled from their appearance until day 11.5 (see Figs 5, 7C, compare to Figs 6, 9C) and then again at day 14.5 (data not shown).

CRABP II, but not CRABP I, transcripts were detected in the meninges covering the brainstem from day 14.5 of gestation (Fig. 8B).

CRABP II transcripts in the hypophysis

From day 12, the anterior hypophysis (adenohypophysis) develops from Rathke's pouch, a dorsal diverticulum of the stomodeal ectoderm, whereas the posterior lobe (neurohypophysis) is derived from the infundibulum of the hypothalamus. CRABP II, but not CRABP I, transcripts were detected in 10.5 day embryos in both Rathke's pouch and in the infundibulum (Fig. 9A). In older embryos, CRABP II transcripts were detected in both neural and endocrine components of the hypophysis at every developmental stage analyzed, whereas no CRABP I transcripts were detected in this structure at any stage (Fig. 9B).

CRABP II transcripts in developing sense organs

At day 9.5, only CRABP II transcripts were detected in the optic vesicles (data not shown). At later stages of development, labelling with both CRABP I and II probes was seen in the neural retina; however, CRABP I transcripts were restricted to the central area of the retina, whereas CRABP II transcripts were homogeneously distributed (Fig. 10A).

The olfactory placodes showed CRABP II, but not CRABP I, transcripts from day 10.5 of development (Fig. 5A, B). At later stages (days 13.5 and 14.5), both the olfactory (oe) and respiratory (re) epithelia still showed abundant CRABP II transcripts (Figs 8A, 10B), whereas CRABP I transcripts were restricted to the olfactory epithelium (Fig. 10B and data not shown, see Dollé et al., 1990). However, the distribution of CRABP I and II transcripts in the olfactory epithelium was different. CRABP II transcripts were detected in both the apical and basal layers of the epithelium, while CRABP I transcripts were preferentially expressed in the middle layer (Fig. 10B). Such a differential labelling could reflect a cell type-specific expression, since at this developmental stage the nuclei of the developing olfactory receptor cells are located medially, while the apical and basal cells are stem cells (Cuschieri and Bannister, 1975).

The internal ear develops from the surface ectoderm-derived otic vesicle or otocyst. CRABP II transcripts were detected in the otocyst from day 9 of development (Fig. 1D). At 13.5 and 14.5 days, transcripts were detected in the inner ear sensory epithelium (data not shown). CRABP I transcripts were transiently expressed in the otic placodes at day 8 of gestation, but no CRABP I transcripts were detected in the otocyst or otocyst-derived

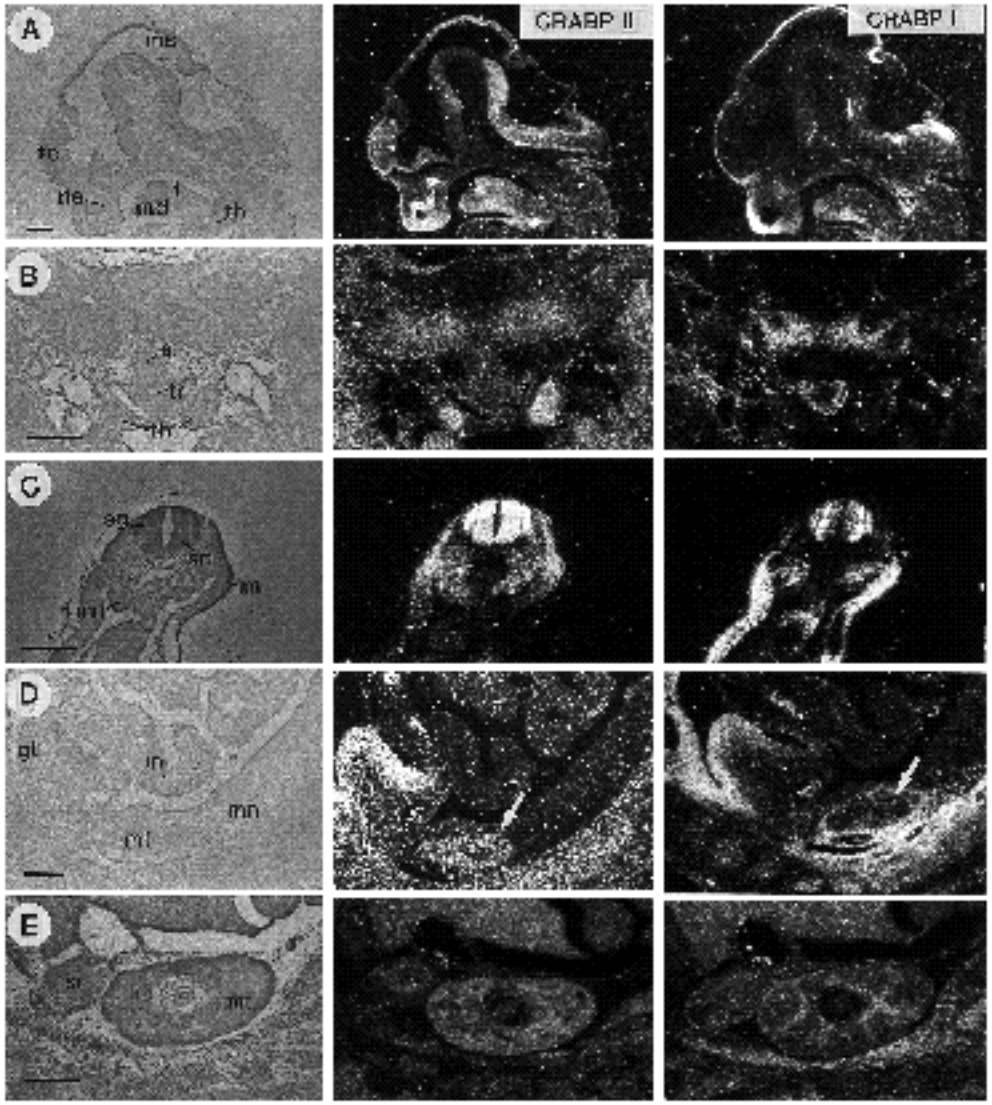

Fig. 7. (A) Parasagittal sections through the head of a 12.5-day embryo to show the signal in the developing thymus with the CRABPII probe. (B) Transverse sections through the thymus of a 13.5-day embryo; only CRABP II transcripts are present. The epithelium of the oesophagus is also labelled with the CRABPII probe, while CRABP I labelling is present in the tracheal mesenchyme. (C) Transverse sections through the nephrotomic region of a 10.5-day embryo. Whereas CRABPII transcripts are detected widely distributed in the mesenchyme and tubules of the mesonephros, CRABPI transcripts are more restricted to the dorsal mesonephric mesenchyme. (D) Parasagittal sections through the developing metanephros at day 12.5 of gestation. The mesonephros is no longer labelled, whereas CRABP II transcripts are now abundant in the metanephric kidney (arrow). Note also the labelling in the periphery of the genital tubercle mesenchyme with both CRABP I and II probes. (E) Sections through the metanephric kidney of a 14.5-day embryo. e, oesophagus; gt, genital tubercle; in, intestine; lm, lateral mesenchyme; md, mandible; mn, mesonephros; ms, mesencephalon; mt, metanephros; ne, nasal epithelium; sc, spinal cord; sg, spinal ganglia; sr, suprarenal gland; t, tongue; te, telencephalon; th, thymus; tr, trachea. Bar, 250μm.

structures in subsequent stages of development (see also Dollé et al., 1990).

Other sites of CRABP II expression

CRABP II transcripts were also detected in the dermal component of the whisker follicles from day 13.5 as well as in dermal component of the skin, which also contained CRABP I transcripts (Fig. 10C, in which the arrows indicate the boundary between the dermis and the epidermis; see also Dollé et al., 1989b, 1990). No CRABP I or II transcripts were seen in the epidermis (Fig.10C and data not shown).

As indicated above, CRABP II transcripts were present in the foregut endoderm from day 8.5 of development (Fig. 1C). From day 10.5 of development a faint signal was detected in the epithelium of the developing stomach (Fig. 5C). Transcripts in the oesophagus (Fig. 7B) and in the stomach epithelium (data not shown) were still found at day 13.5 of development. The gut epithelium showed no CRABP transcripts at any stage analyzed (Fig. 7D and data not shown); in contrast, CRABP I, but not CRABP II, labelling was observed in the mesenchyme of the stomach close to the dorsal mesentery from day 10.5 of gestation (Fig. 5C). CRABP I and II transcripts were also detected

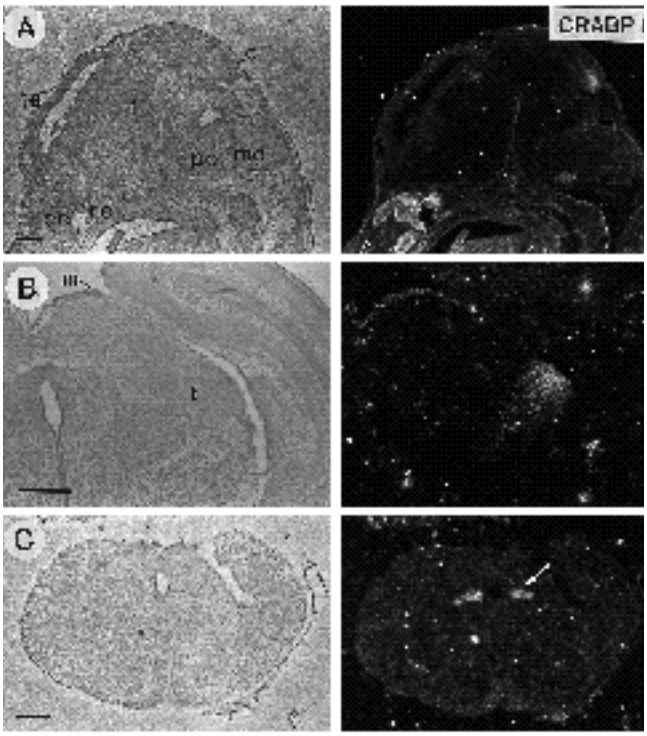

Fig. 8. (A) Parasagittal section through the head of a 14.5-day embryo hybridized with the CRABP II probe. Transcripts are detected in the thalamus and pontine region. (B) Coronal section through the brain of an 18.5-day fetus, in which CRABP II transcripts are found in the thalamus. (C) Coronal section through the lower medulla oblongata at the level of the dorsal efferent nucleus of the vagus (arrow). c, colliculi; m, meninges; mo, medulla oblongata; oe, olfactory epithelium; po, pons; re, respiratory epithelium; t, thalamus; te, telencephalon. Bar, 500μm.

in the developing teeth, in both the epithelium and mesenchyme (not shown, see also Mark et al., 1991). Low levels of CRABP II, but no CRABP I, transcripts were detected in the liver (Fig. 6 and data not shown). At the stages analyzed, no labelling above the background was seen in the lung epithelium with either CRABP I or II probes, but CRABP I transcripts were detected in the mesenchyme surrounding the trachea (Fig. 7B, see also Dollé et al., 1990).

Discussion

We have described here the distribution of CRABP II transcripts during mouse embryogenesis and compared it with that of CRABP I. The widespread distribution of these transcripts during morphogenesis suggests that both CRABPs have essential functions in the processes involved in transducing the RA signal in normal development. However, our results (summarized in Table 1) reveal specific patterns of spatio-temporal distribution, suggesting that the two CRABPs play different functions within the cells of developing embryos. There is increasing evidence that CRABP I may be involved in the control of the levels of free RA that are available to the nuclear receptors. Firstly, RA-induced differentiation of F9 cells, and RA-induced expression of RAR-β, are reduced by 80-90% in F9 cells that express elevated levels of functional CRABP I protein (Boylan and Gudas, 1991). Secondly, in embryonic tissues, there is a clear correlation between vulnerability to RA excess and the localization of CRABP I (Dollé et al., 1990; Dencker et al., 1990; Vaessen et al., 1990; Ruberte et al., 1991), suggesting that cells expressing CRABP I are unable to develop normally when free RA levels are raised. The embryonic structures that express CRABP II transcripts similarly

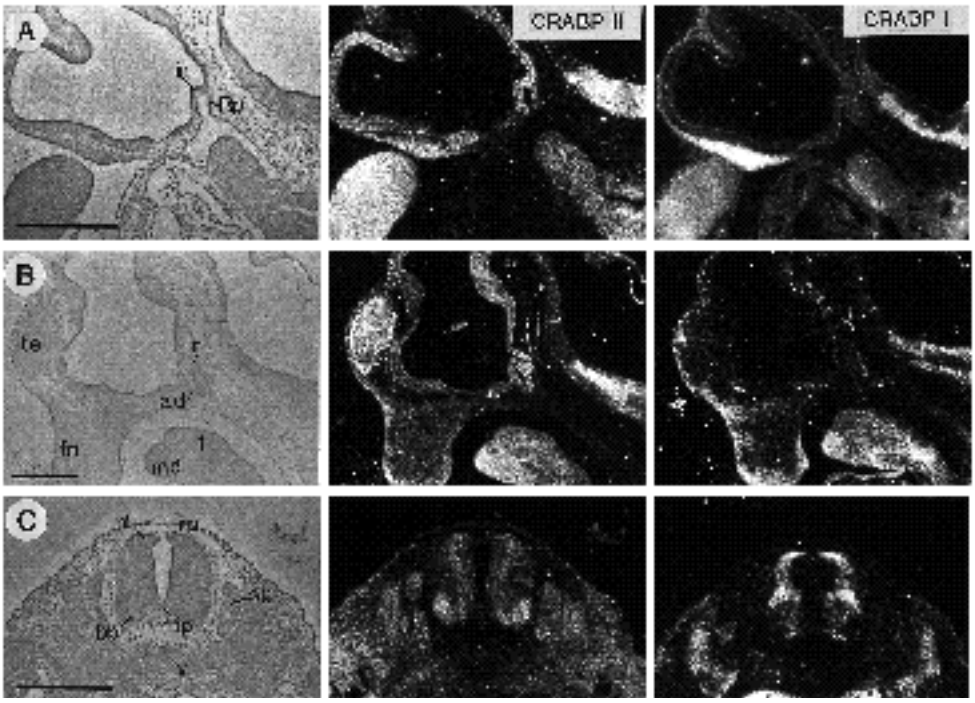

Fig. 9. (A and B) Parasagittal sections through the head of 10.5 and 12.5 day embryos, respectively, to show the labelling of both components of the hypophysis with the CRABP II probe. (C) Transverse sections through the spinal cord of a 13.5-day embryo. CRABP II transcripts are detected preferentially in the columns of motoneurons in the basal plate, whereas CRABP I transcripts are preferentially found in the alar plate. ad, adenohypophysis; bp, basal plate; fn, frontonasal mass; fp, floor plate; in, infundibulum; md, mandible; n, neurohypophysis; nl, neuroepithelial layer; Rp, Rathke's pouch; rp, roof plate; sg, spinal ganglion; t, tongue; te, telencephalon; v, vertebra; Bar, 250 μm.

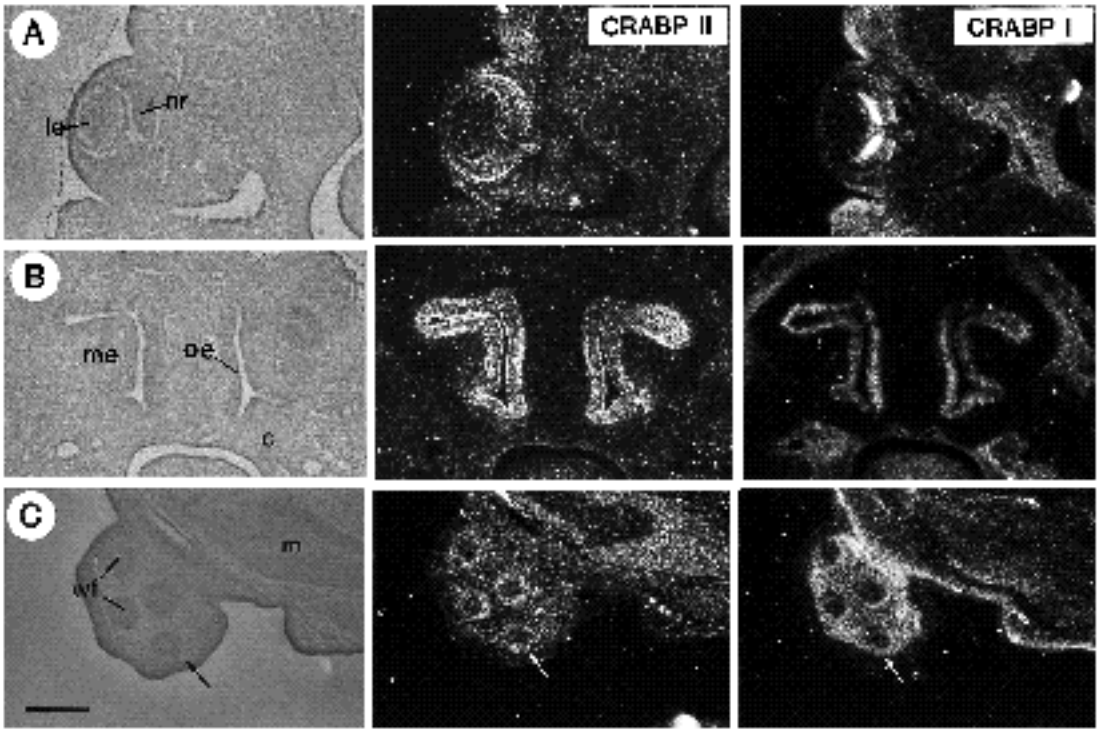

Fig. 10. (A) Transverse sections through the eye at 13.5 days of gestation, showing labelling in the neural retina with both CRABPI and II probes. (B) At day 13.5 of development CRABPI and II transcripts show different patterns within the nasal epithelium. (C) Parasagittal sections of the head of a 13.5-day embryo to illustrate the labelling in the mesenchymal component of the whisker follicles and the differential labelling of the dermis and epidermis with the CRABP I and II probes. Arrows mark the boundary between the dermis and the epidermis. c, cartilage; le, lens; m, muscle; me, mesenchyme; nr, neural retina; oe, olfactory epithelium; wf,whisker follicles.Bar, 500 μm.

include structures whose development has been shown to be affected by excess of retinoids, such as the limbs, hindbrain and cranial neural crest cells, but this gene is also expressed in tissues not known to be specifically sensitive to RA excess.

CRABP expression and the presence of RA

RAR-β, CRBP I and CRABP II are RA-inducible and contain RAREs in their promoter region (de Thé et al., 1990; Mendelsohn et al., 1991; Smith et al., 1991; B. Durand and P. Chambon, unpublished results from our laboratory). Interestingly, CRABP II, RAR-β and CRBP I transcripts are co-expressed in a number of embryonic structures suggesting a link between the synthesis of RA from retinol and the transcriptional regulation of a subsets of RA-responsive genes. Among the structures coexpressing RAR-β, CRABP II and CRBP I genes are the gut endoderm and its derivatives, the metanephric kidney, the hypophysis, the meninges and interdigital mesenchyme, all of which are devoid of CRABP I transcripts, thus suggesting that CRABP II, RAR-β and CRBP I could be involved in a common RA-induced morphogenetic mechanism.

However, CRABP II is also expressed in sites lacking CRBP I and/or RAR-β expression, such as the major part of the limb bud mesenchyme (which in contrast expresses also CRABP I) and hindbrain neuroepithelim, indicating that, in contrast to what has been recently assumed (Noji et al., 1991), the presence or absence of RA in a given site cannot be validly deduced from the presence or absence of the transcripts of a given RA-inducible gene (for a further discussion of this point see Ruberte et al., 1992). Whether a particular RA-responsive gene is in fact poised for transcription in that given site is certainly a prerequisite to observe induction of its expression by RA.

CRABP I and CRABP II expression in the hindbrain and its derived neural crest

The formation of rhombomeric divisions in the hindbrain neuroepithelium during neurulation was accompanied by a changing pattern of expression of CRABP I and CRABP II. This pattern showed different levels of intensity of transcripts at different stages and in different locations, and was clearly rhombomere-related. The appearance at three stages of development is illustrated in Fig. 11A.

Many other genes have been shown to have changing patterns of expression during the process of hindbrain segmentation in mouse embryos, as indicated in Fig. 11B (Wilkinson et al., 1988; Murphy et al., 1989; Wilkinson et al., 1989a, 1989b; Hunt et al., 1991; Murphy and Hill,1991; Ruberte et al., 1991). In embryos exposed to RA excess prior to the onset of morphological segmentation, normal rhombomere formation is suppressed and the normal pattern of segment-specific expression domains of Hox-2.9 and Krox-20 fails to develop (Morriss-Kay et al., 1991). The particular RA-sensitivity of the segmented part of the hindbrain and its derived neural crest indicates that both normal

Table 1. *Diagrammatic transcript distribution of CRABP in mouse embryonic structures*

	CRABP I	CRABP II
Ectoderm derivates		
neuroepithelium	❊	+
telencephalon	−	+
mesencephalon	❊	+
metencephalon	+	+
myelencephalon	+	+
spinal cord	+	+
ganglia	+	+
neural crest	+	❊
olfactory epithelium	❊	+
respiratory epithelium	−	+
eye (neural retina)	+	+
internal ear	−	+
epidermis	−	−
neurohypophysis	−	+
Mesoderm derivates		
somatopleure	+	+
splanchnopleure	−	−
pharyngeal arch mesenchyme	+	❊
somites	❊	+
limbs mesenchyme	+	+
thymus	−	+
digestive tube mesenchyme	❊	−
heart	❊	−
metanephros	+	+
genital tubercle	+	+
dermis	+	+
meninges	−	+
Endoderm derivates		
pharyngeal pouches	−	+
oesophagus	−	+
intestine	−	−
lungs	−	−
tracheal epithelium	−	+
liver	−	+
adenohypophysis	−	+

(+) and (−) indicate the presence or absence, respectively, of the corresponding transcripts. ❊ indicates that the presence of transcripts is spatially and/or temporally restricted.

rhombomere formation and the normal pattern of segmental gene expression in this region depend on restriction of the access of free RA to the nuclear receptors. We have already proposed that RA binding to CRABP I is involved in this regulation (Dollé et al., 1990; Ruberte et al., 1991). The present observations, and those previously reported for the hindbrain domain of expression of CRABP I (Ruberte et al., 1991), indicate that CRABP I is expressed in appropriate positions and at appropriate stages in order to play this role. Furthermore, the present observations strongly suggest that CRABP II is also involved in the process of hindbrain segmentation, since it is expressed in a changing segment-related pattern. Both CRABPs continue to be expressed in a segment-related pattern when rhombomere formation is complete, so may be important for the maintenance of segmentation.

The differential pattern of CRABP transcription in the hindbrain is also relevant to rhombomere-specific contributions to the neural crest. In mammalian embryos, cranial neural crest cell migration begins at the prerhombomere stage when the neural cranial folds are widely open and convex in form (Müller and O'Rahilly, 1985; Nichols, 1981; Tan and Morriss-Kay, 1986). These early crest cells, which migrate into the pharyngeal arches (Tan and Morriss-Kay, 1986), show strong labelling with the CRABP I probe, but are only faintly labelled for CRABP II. After the formation of rhombomeres, a second population of crest cells emigrates to form the cranial ganglia; unlike the mesenchymal cells, the preganglionic crest cells show high levels of both CRABP I and II transcripts. They emigrate from the hindbrain neuroepithelium in a rostrocaudal sequence as three populations separated by rhombomeres 3 and 5, from which crest cells do not migrate (except perhaps for a small Krox-20-expressing group from the caudal edge of rhombomere 5; see Morriss-Kay et al., 1991). It is therefore interesting to note that the lowest level of expression of CRABP I is in rhombomere 3 (18-19 somite stage), while that of CRABP II is in rhombomere 5 (11-12 somite stage). It is also noteworthy that rhombomere 4, which displays the highest levels of CRABP I and II transcripts, is the site of origin of the cranial facial (VII) nerve, the development of which is adversely affected by an excess of retinoids, both in human (Lammer et al., 1985) and mouse (unpublished results from our laboratory).

CRABP I and II in the limbs

RA appears to play an important role in vertebrate limb morphogenesis. Two mechanisms of action have been suggested: according to the first one, RA is released by the zone of polarizing activity (ZPA) and acts as a diffusible morphogen conferring positional values through the anteroposterior axis of the limb; alternatively, RA may act as a local inducer of the morphogen (for references and a review, see Tabin, 1991; Brockes, 1991).

We have studied the distribution of CRABP I and II transcripts in serial sections of the developing limbs and found that they are not homogeneously distributed through the limb bud mesenchyme. At day 10.5, CRABP I transcripts are more abundant in the posterior region, and almost absent from the proximal dorsal anterior region, whereas CRABP II transcripts appear more abundant in the dorsal than in the ventral part of the limb mesenchyme. Moreover the rapidly proliferating cells located at the tip of the limb buds (progress zone, Summerbell and Lewis, 1975), which contain high levels of CRABP I transcripts (see also Dollé et al., 1989b), show only a weak signal with the CRABP II probe. If the role of these binding proteins is, as has been suggested, to control the levels of RA available to bind to the nuclear receptors, it is interesting to note that the overlapping of the two patterns of transcript distribution would not result in a gradient of free retinoic acid, but in a complicated pattern of local RA levels along the three axes of the limb bud. Interpretation of the roles of the two RA binding proteins in the progress zone is further complicated by the observation that their relative labelling intensities are reversed by day 13.5.

Homeogenes are likely candidates for the interpretation of RA signals in the limb, since at least some homeogenes have been shown to respond to RA both in cultured EC cells in vitro (Mavilio et al., 1988; Simeone et al., 1990, 1991; Papalopulu et al., 1991) and in vivo (Izpisúa-Belmonte et al., 1991; Nohno et al., 1991). A number of Hox-4 genes have a uniquely restricted expression domain in the

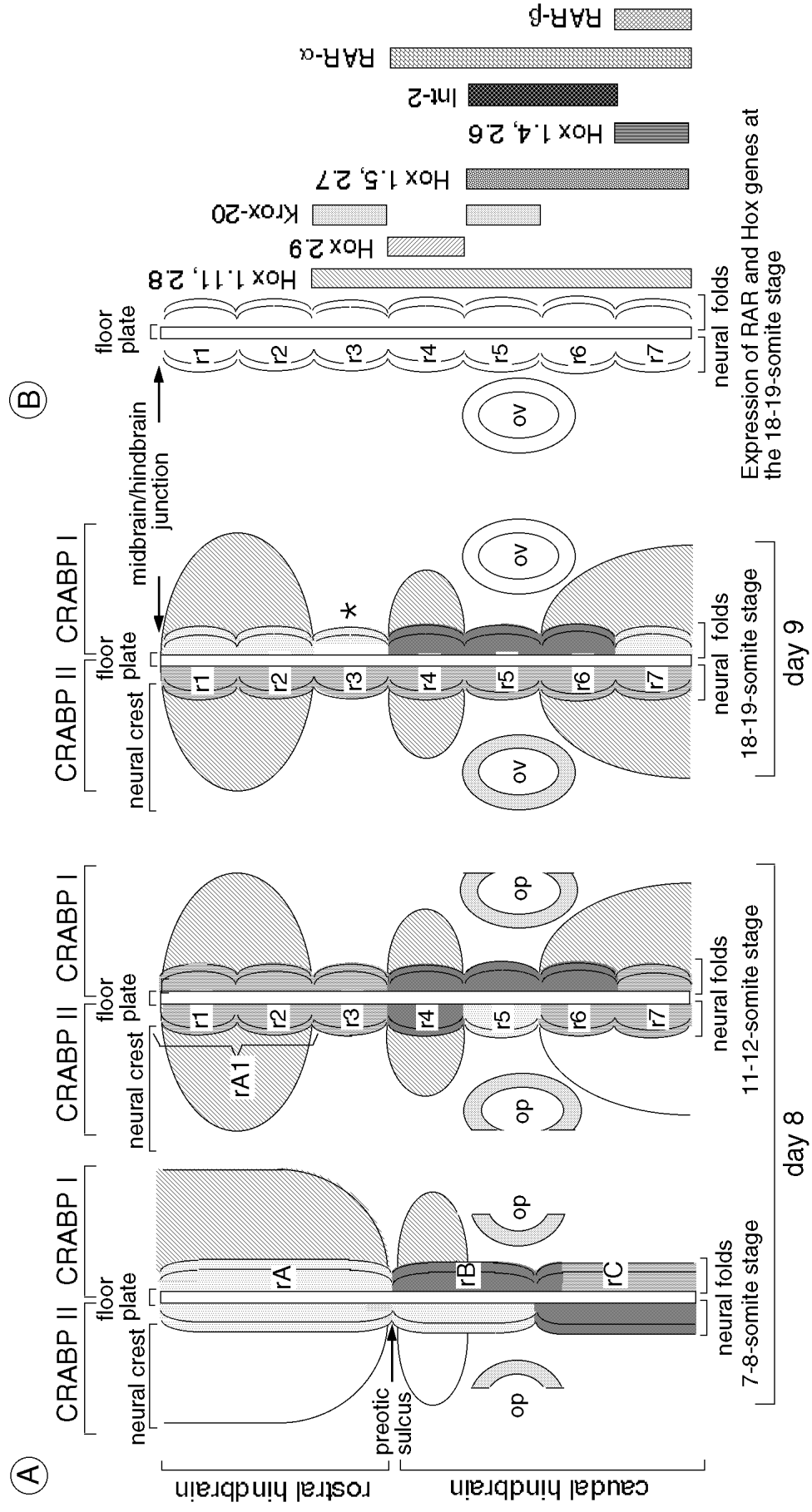

Fig. 11. (A) Diagrammatic representation of the transcript distribution of CRABP I and II at three different times of development in the hindbrain. The migrating cranial neural crest cells are represented. The shading reflects the presence of transcripts, and within the rhombomeres, the increasing shading intensities correspond to increasing amounts of transcripts. The asterisk means that the transcripts are not homogeneously distributed through the neural epithelium. (B) Diagrammatic representation of the transcript distribution of the retinoic acid receptors and some other developmental genes in the rhombomeres at day 9 of gestation (see text). op, otic placode; ov, otic vesicle.

posterior part of the developing mouse (Dollé et al., 1989a) and chick (Nohno et al., 1991) limb, which is related to their position in the Hox-4 complex. Moreover, there is a sequential triggering of expression of these Hox-4 genes from the postero-dorsal region of the limb, which apparently coincides with the ZPA. There is also a graded expression of each gene along the anteroposterior axis, which is highest in the posterior region and decreases anteriorly. Strikingly, grafting a ZPA in, or a local application of RA to the anterior margin of chick wing buds, results in mirror-image patterns of Hox-4 gene expression which correlate with the subsequent appearence of mirror-image duplications of digits (Izpisúa-Belmonte et al., 1991; Nohno et al., 1991). These results are consistent with the idea that RA is involved in controlling the expression of the Hox-4 complex. Interestingly, there is a maximal overlap of expression of the two CRABP genes in the postero-dorsal region which corresponds to the region of appearance of Hox-4 gene expression. Recently some of the Hox-1 genes have also been shown to have colinear spatial and temporal patterns of transcription along the proximo-distal axis of the limbs (Yokouchi et al., 1991). The site of appearance of their expression in the distal portion of the limbs corresponds to the region of highest CRABP I expression and lowest CRABP II expression.

Whether and how the RA binding proteins are involved in RA-induced expression of the Hox-4 and Hox-1 complex genes during limb development will require the generation of mice in which the expression of CRABP I and II has been altered. Their continuous expression at stages after the skeletal pattern is established suggests that they are also important for differentiation and histogenesis of the non-skeletal tissues of the limb, as well as elsewhere in the body.

We are grateful to Drs P. Kastner, C. Stoner, L. Gudas, A. Krust and P. Leroy for generous gifts of probes. We thank all the members of the retinoic acid receptor group for useful discussions, C. Werlé, A. Landmann, B. Boulay and J.M. Lafontaine for illustrations, and the secretarial staff. This work was supported by the INSERM, the CNRS, the Centre Hospitalier Universitaire Régional, the Human Frontier Science Program, the Fondation pour la Recherche Médicale and the Association pour la Recherche sur le Cancer. E.R. was supported by a fellowship from the Université Louis Pasteur.

References

Adelmann, H. B. (1925). The development of the neural folds and cranial ganglia of the rat. *J.comp. Embryol.* **39,** 19-171.

Bartelmez, G. W. (1923). The subdivisions of the neural folds in man. *J. Comp. Neurol.* **35,** 231-247.

Benbrook, D., Lernhardt, E. and Pfahl, M. (1988). A new retinoic acid receptor from a hepatocellular carcinoma. *Nature* **333,** 669-672.

Blomhoff, R., Gree, M. H., Berg, T. and Norum, K. R. (1990). Transport and storage of vitamin A. *Science* **250,** 339-404.

Boylan, J. F. and Gudas, L. J. (1991). Overexpression of the cellular retinoic acid binding protein-I (CRABP-I) results in a reduction in differentiation-specific gene expression in F9 teratocarcinoma cells. *J.Cell Biol.* **112,** 965-979.

Brand, N., Petkovich, M., Krust, A., Chambon, P., de Thé, H., Marchio, A., Tiollais, P. and Dejean, A. (1988). Identification of a second human retinoic acid receptor. *Nature* **332,** 850-853.

Brockes, J. (1991). We may not have a morphogen. *Nature* **350,** 15.

Chytil, F. and Stump, D. G. (1991). Cellular retinoic acid- and retinol-binding proteins.In *Retinoids: 10 years on.*, (ed. J. H. Saurat), pp.38-45. Basel : Karger.

Couly, G. and Le Douarin, N. M. (1987). Mapping of the early neural primordium in quail-chick chimeras. II. The prosencephalic neural plate and neural folds: implications for the genesis of cephalic human congenital abnormalities. *Devl. Biol.* **120,** 198-214.

Cuschieri, A. and Bannister, L. H. (1975). The development of the olfactory mucosa in the mouse: light microscopy. *J. Anat.* **119,** 277-286.

Dencker, L., Annerwall, E., Busch, C. and Eriksson, U. (1990). Localization of specific retinoid-binding sites and expression of cellular retinoic-acid binding protein (CRABP) in the early mouse embryo. *Development* **110,** 343-352.

de Thé, H., Vivanco Ruiz, M. M., Tiollais, P., Stunnenberg, H. and Dejean, A. (1990). Identification of a retinoic acid responsive element in the retinoic acid receptor β gene. *Nature* **343,** 177-180.

Dollé, P., Izpisua-Belmonte, J. C., Falkenstein, H., Renucci, A. and Duboule, D. (1989a). Coordinate expression of the murine Hox-5 complex homeobox-containing genes during limb pattern formation. *Nature* **342,** 767-772.

Dollé, P., Ruberte, E., Kastner, P., Petkovich, M., Stoner, C. M., Gudas, L. J. and Chambon, P. (1989b). Differential expression of the genes encoding the retinoic acid receptors α, β, γ and CRABP I in the developing limbs of the mouse. *Nature* **342**, 702-705.

Dollé, P., Ruberte, E., Leroy, P., Morriss-Kay, G. M. and Chambon, P. (1990). Retinoic acid receptors and cellular retinoid binding proteins. I. A systematic study of their differential pattern of transcription during mouse organogenesis. *Development* **110**, 1133-1151.

Giguère, V., Lyn, S., Yip, P., Siu, C. H. and Evans, R. M. (1990). Molecular cloning of cDNA encoding a second cellular retinoic acid-binding protein. *Proc. Natl. Acad. Sci. USA* **87**, 6233-6237.

Giguère, V., Ong, E. S., Segui, P. and Evans, R. M. (1987). Identification of a receptor for the morphogen retinoic acid. *Nature* **330**, 624-629.

Hunt, P., Faiella, A., Cook, M., Sham, M-H., Gulisano, M., Wilkinson, D., Boncinelli, E. and Krumlauf, R. (1991). A distinct Hox code for the branchial region of the head. *Nature* **353**, 861-864.

Izpisúa-Belmonte, J.-C., Tickle, C., Dollé, P., Wolpert, L. and Duboule, D. (1991). Expression of the homeobox Hox-4 genes and specification of position in chick wing development. *Nature* **350**, 585-589.

Krust, A., Kastner, P., Petkovich, M., Zelent, A. and Chambon, P. (1989). A third human retinoic acid receptor, h RAR-γ. *Proc. Natl. Acad. Sci. USA* **86**, 5310-5314.

Lammer, G. J., Chen, D. T., Hoar, R. M., Agnish, N. D., Benke, P. J., Braun, J. T., Curry, C. J., Fernhoff, P. M., Grix, A. W., Lott, I. T., Richard, J. M. and Sun, S. C. (1985). Retinoic acid embryopathy. *New England J. Med.* **333**, 837-841.

Maden, M., Ong, D. E., Summerbell, D. and Chytil, F. (1988). Spatial distribution of cellular protein binding to retinoic acid in the chick limb bud. *Nature* **335**, 733-735.

Mark, M. P., Bloch-Zupan, A., Wolf, C., Ruberte, E. and Ruch, J. V. (1991). Involvement of cellular retinoic acid-binding proteins I and II (CRABP I and CRABP II) and of the cellular retinol-binding protein I (CRBP) in odontogenesis in the mouse. *Differentiation* **48**, 89-98.

Mavilio, F., Simeone, A., Boncinelli, E. and Andrews, P. W. (1988). Activation of four homeobox gene clusters in human embryonal carcinoma cells induced to differentiate by retinoic acid. *Differentiation* **37**, 73-79.

Mendelsohn, C., Ruberte, E., LeMeur, M., Morriss-Kay, G. and Chambon, P. (1991). Developmental analysis of the retinoic acid inducible RAR-β2 promoter in transgenic animals. *Development* 723-734.

Morriss, G. M. (1972). Morphogenesis of the malformations induced in rat embryos by maternal hypervitaminosis A. *J. Anat.* **113**, 241-250.

Morriss-Kay, G. M., Murphy, P., Davidson, D. R. and Hill, R. E. (1991). Effects of retinoic acid excess on expression of Hox-2.9 and Krox-20 and on morphological segmentation in the hindbrain of mouse embryos. *EMBO J.* **10**, 2985-2995

Müller, F. and O'Rahilly, R. (1985). The first appearance of the neural tube and optic primordium in the human embryo at stage 10. *Anat. Embryol.* **172**, 157-169.

Murphy, P., Davidson, D. R. and Hill, R. E. (1989). Segment-specific

expression of a homeobox-containing gene in the mouse hindbrain. *Nature* **341**, 156-159.

Murphy, P. and Hill, R. E. (1991). Expression of the mouse labial-like homeobox containing genes, Hox 2.9 and Hox 1.6, during segmentation of the hindbrain. *Development* **111**, 61-74.

Nichols, D. H. (1981). Neural crest formation in the head of the mouse embryo as observed using a new histological technique. *J. Embryol. exp. Morph.* **64**, 105-120.

Noden, D. M. (1978a). The control of avian cephalic neural crest cytodifferentiation. I. Skeletal and connective tissues. *Dev. Biol.* **67**, 296-312.

Noden, D. M. (1978b). The control of avian cephalic neural crest cytodifferentiation. II. Neural tissues. *Dev. Biol.* **67**, 313-329.

Nohno, T., Noji, S., Koyama, E., Ohyama, K., Myokai, F., Kuroiwa, A., Saito, T. and Taniguchi, S. (1991). Involvement of the Chox-4 chicken homeobox genes in determination of anteroposterior axial polarity during limb development. *Cell* **64**, 1197-1205.

Noji, S., Nohno, T., Koyama, E., Muto, K., Ohyama, K., Aoki, Y., Tamura, K., Ohsugi, K., Ide, H., Taniguchi, S. and Saito, T. (1991). Retinoic acid induces polarising activity but is unlikely to be a morphogen in the chick limb bud. *Nature* **350**, 83-86.

O'Rahilly, R. and Müller, F. (1987). In *Developmental Stages in Human Embryos*, Publication 637. (ed. Carnegie Institution of Washington).

Papalopulu, N., Lovell-Badge, R., and Krumlauf, R. (1991). The expression of murine Hox-2 genes is dependent on the differentiation pathway and displays a collinear sensitivity to retinoic acid in F9 cells and *Xenopus* embryos. *Nucl. Acids Res.* **19**, 5497-5506.

Petkovich, M., Brand, N. J., Krust, A. and Chambon, P. (1987). A human retinoic acid receptor which belongs to the family of nuclear receptors. *Nature* **330**, 444-450.

Robertson, M. (1987). Towards a biochemistry of morphogenesis. *Nature* **330**, 420-421.

Rosa, F. W., Wilk, A. L. and Kelsey, F. O. (1986). Teratogen update: vitamin A congeners. *Teratology* **33**, 355-364.

Ruberte, E., Dollé, P., Chambon, P. and Morriss-Kay, G. (1991). Retinoic acid receptors and cellular retinoid binding proteins II. Their differential pattern of transcription during early morphogenesis in mouse embryos. *Development* **111**, 45-60.

Ruberte, E., Dollé, P., Krust, A., Zelent, A., Morriss-Kay, G. and Chambon, P. (1990). Specific spatial and temporal distribution of retinoic acid receptor gamma transcripts during mouse embryogenesis. *Development* **108**, 213-222.

Ruberte, E., Nakshatri, H., Kastner, Ph. and Chambon, P. (1992). Retinoic acid receptors and binding proteins in mouse limb development. In *Retinoids in Normal Development and Teratogenesis*. (ed. G. M. Morriss-Kay) pp. 99-111. Oxford: Oxford University Press.

Shenefelt, R. E. (1972). Morphogenesis of malformations in hamster caused by retinoic acid, relation to dose and stage at treatment. *Teratology* **5**, 103-108.

Simeone, A., Acampora, D., Arcioni, L., Andrews, P. W., Boncinelli, E. and Mavilio, F. (1990). Sequential activation of human HOX-2 homeobox genes by retinoic acid in embryonal carcinoma cells. *Nature* **346**, 763-766.

Simeone, D., Acampora, V., Nigro, A., Faiella, M., D'Esposito, A., Stornaiuolo, F., Mavilio, F. and Boncinelli, E. (1991). Differential regulation by retinoic acid of the homeobox genes of the four HOX loci in human embryonal carcinoma cells. *Mech. of Dev.* **33**, 215-227.

Smith, S. M., Pang, K., Sundin, O., Wedden, S. E., Thaller, C. and Eichele, G. (1989). Molecular approaches to vertebrate limb morphogenesis. *Development* **107 (suppl.)**, 121-131.

Smith, W. C., Nakshatri, H., Leroy, P., Rees, J. and Chambon, P. (1991). A retinoic acid response element is present in the mouse cellular retinol binding protein I (mCRBP I) promoter. *EMBO J* **10**, 2223-2230

Stoner, C. M. and Gudas, L. J. (1989). Mouse cellular retinoic acid binding protein: cloning, complementary DNA sequence, and messenger RNA expression during the retinoic acid induced differentiation of F9 wild type and RA-3-10 mutant teratocarcinoma. *Cancer Research* **49**, 1497-1504.

Summerbell, D. and Lewis, J. H. (1975). Time, place and positional value in the chick limb-bud. *J. Embryol. exp. Morph.* **33**, 621-643.

Tabin, C. J. (1991). Retinoids, homeoboxes, and growth factors: towards molecular models for limb development. *Cell* **66**, 199-217.

Takase, S., Ong, D. E. and Chytil, F. (1979). Cellular retinol-binding protein allows specific interaction of retinol with the nucleus in vitro. *Proc. Natl. Acad. Sci. USA*., **76**, 2204-2208.

Takase, S., Ong, D. E. and Chytil, F. (1986). Transfer of RA from its complex with cellular retinoic acid binding protein to the nucleus. *Arch. Biochem. Biophys.* **247,** 328.

Tan, S. S. and Morriss-Kay, G. M. (1986). Analysis of cranial neural crest cell migration and early fates in postimplantation rat chimeras. *J. Embryol. exp. Morph.* **98**, 21-58.

Vaessen, M. J., Meijers, J. H. C., Bootsma, D. and van Kessel, A. G. (1990). The cellular retinoid binding protein is expressed in tissues associated with retinoic acid induced malformations. *Development* **110**, 371-378.

Warkany, J., Nelson, R. C. and Schraffenberger, E. (1943). Congenital malformations induced in rats by maternal nutritional deficiency. III. The malformations of the extremities. *J. Bone and Joint Surg.* **5**, 261-270.

Wilkinson, D. G., Bhatt, S., Chavrier, P., Bravo, R. and Charnay, P. (1989a). Segment-specific expression of a zinc-finger gene in the developing nervous system of the mouse. *Nature* **337**, 461-464.

Wilkinson, D. G., Bhatt, S., Cook, M., Boncinelli, E. and Krumlauf, R. (1989b). Segmental expression of Hox-2 homeobox containing genes in the developing mouse hindbrain. *Nature* **341**, 405-409.

Wilkinson, D. G., Peters, G., Dickson, C. and MacMahon, A. P. (1988). Expression of the FGF-related proto-oncogene int-2 during gastrulation and neurulation in the mouse. *EMBO J.* **7**, 691-695.

Wilson, J. G., Roth, C. B. and Warkany, J. (1953). An analysis of the syndrome of malformations induced by maternal vitamin A deficiency. Effects of restoration at various times during gestation. *Am. J. Anat.* **92**, 189-217.

Yokouchi, Y., Sasaki, H. and Kuroiwa, A. (1991). Homeobox expression correlated with the bifurcation process of limb cartilage development. *Nature* **353**, 443-445.

Zelent, A., Krust, A., Petkovich, M., Kastner, P. and Chambon, P. (1989). Cloning of murine α and β retinoic acid receptors and a novel receptor γ predominantly expressed in the skin. *Nature* **339**, 714-717.

(*Accepted 24 April 1992*)